Hyperon/meson ratios in rare high-multiplicity pp collisions at energies available at the Large Hadron Collider, and potential signatures for mini-quark-gluon plasma formation

V. Topor Pop, M. Gyulassy, J. Barrette, C. Gale, and A. Warburton

Phys. Rev. C **86**, 044902 — Published 12 October 2012

DOI: 10.1103/PhysRevC.86.044902

Hyperon/meson ratios in rare high-multiplicity pp collisions at energies available at the Large Hadron Collider, and potential signatures for mini-quark-gluon plasma formation

V. Topor Pop,[1] M. Gyulassy,[2] J. Barrette,[1] C. Gale,[1] and A. Warburton[1]

[1] *McGill University, Montreal, Canada, H3A 2T8*

[2] *Columbia University, New York, N.Y. 10027*

Abstract

We use the framework of the HIJING/B$\bar{\text{B}}$ v2.0 model to simulate high-multiplicity (HM) $p+p$ collision events at the Large Hadron Collider (LHC) to study observables sensitive to possible collective phenomena, such as strong longitudinal color fields (SLCF) modeled by an enhanced string tension (κ). We focus on the hyperon/meson yield ratios at center-of-mass (c.m.) energy $\sqrt{s}$ = 7 TeV, in the transverse momentum region, $1 < p_T < 4$ GeV/c. For minimum bias events these ratios are well described assuming an energy dependence $\kappa = \kappa(s) = \kappa_0(s/s_0)^{0.04}$ GeV/fm (κ_0= 1 GeV/fm), giving a value $\kappa = 2$ GeV/fm at $\sqrt{s}$ = 7 TeV. We compare minimum bias (MB) events to simulated HM events assuming that $\kappa(MB) = 2$ GeV/fm could grow to an extreme value of $\kappa(HM) = 5$ GeV/fm that saturates the strangeness suppression factor. With this assumption the model predicts a very strong enhancement of (multi)strange baryon/meson ratios in HM events. If observed, such an enhancement could be also interpreted as a possible signature for formation in HM $p+p$ collision events of a deconfined but out of local thermal equilibrium *mini quark-gluon plasma* (mQGP).

PACS numbers: 12.38.Mh, 24.85.+p, 25.40Ve, 25.75.-q

I. INTRODUCTION

Charged particle multiplicities measured in high-multiplicity (HM) $p + p$ collisions at CERN Large Hadron Collider (LHC) energies reach values that are of the same order as those measured in heavy-ion collisions at lower energies (*e.g.*, well above those observed at RHIC for Cu + Cu collisions at $\sqrt{s_{\rm NN}} = 200$ GeV [1]). The Bjorken energy density relation [2] connects high multiplicity events with high energy density. Within that approach at the LHC, $p + p$ collisions could reach an energy density of 5-10 GeV/fm^3, comparable to those in $A + A$ collisions at RHIC [3]. It is, therefore, a valid question whether $p + p$ collisions also exhibit any behavior of the kind observed in heavy-ion collisions [4–11]. Bjorken first suggested the idea of possible deconfinement in $p+p$ collisions [4]. It has also been suggested by Van Hove [12] and recently by Campanini [13] that an anomalous behavior of average transverse momentum ($< p_T >$) as a function of multiplicity could be a signal for the occurrence of a phase transition in hadronic matter, *i.e.*, formation of a *mini quark-gluon plasma* (mQGP). The hadronic interaction model EPOS (Partons Off-shell remnants and Splitting of parton ladders), has also been used to describe the production of mQGP features in high energy density $p + p$ collisions [14, 15].

Another indication of collective phenomena might be the observed long-range, near-side angular correlation (ridge) in HM $p + p$ collisions at center-of-mass energy $\sqrt{s} = 7$ TeV for charged particle multiplicities well above the mean multiplicity. CMS [16–18] and ATLAS [19] constructed a two-particle correlation function and measured its value for different $\Delta\eta$ and $\Delta\Phi$ angular separations. When looking at particles in a specific range of p_T and high multiplicity ($1 < p_T < 3$ GeV/c and $N_{\rm ch} > 110$), a clear ridge-like structure emerges at $\Delta\Phi \approx 0$ and $2 < |\Delta\eta| < 4.8$, that is not reproduced by existing Monte Carlo (MC) event generators [16]. The origin of this unexpected *ridge-like* structure found in the two-particle correlation analysis, albeit attracting much theoretical attention, is still under debate [20–25].

Identified particle production has been studied in detail by the ATLAS [26], ALICE [27–32] and CMS [33–35] collaborations in $p + p$ collisions at the LHC. Meson (π, K, K^0_S) and baryon (p, Λ, Ξ^-, Ω) yields, rapidity and multiplicity distributions have been measured with different event selections [minimum bias, inelastic (INEL) or non-single diffractive events (NSD)]. For minimum bias event selection, different PYTHIA parameter sets [36–39] have difficulty reproducing (multi)strange particle production, predicting too few strange particles and harder p_T spectra, the differences with data increasing with the mass of the strange particle [34]. Up to now, none of the MC event generators is able to describe the softer p_T and the huge rise of particle production with energy. This has led to a concerted effort to improve the available MC generators.

In a string fragmentation phenomenology, it has been proposed that the observed strong enhancement of strange particle production in nuclear collisions could be naturally explained via strong longitudinal color field effects (SLCF) [40]. Recently, an extension of Color Glass Condensate (CGC) theory has proposed a more detailed dynamical "GLASMA" model [41, 42] of color ropes. In the string models, strong longitudinal fields (flux tubes, effective strings) decay into new ones by quark anti-quark ($q\bar{q}$) or diquark anti-diquark (qq-$\overline{\mathrm{qq}}$) pair production and subsequently hadronize to produce the observed hadrons. Due to confinement, the color of these strings is restricted to a small area in transverse space. With increasing energy of the colliding particles, the number of strings grows and they start to overlap, forming clusters This can introduce a possible dependence of particle production on the energy density [11].

We have studied [48] the effect of strong longitudinal color fields (SLCF) in $p+p$ collisions up to LHC energies in the framework of the HIJING/B$\bar{\mathrm{B}}$ v2.0 model, which combines (collinear factorized) pQCD multiple minijet production with soft longitudinal string excitation and hadronization. The default vacuum string tension, $\kappa_0 = 1$ GeV/fm, is replaced by an effective energy dependent string tension, $\kappa(s) = \kappa_0(s/s_0)^{0.06}$ GeV/fm that increases monotonically with center-of-mass energy. The exponent $\lambda = 0.06$ is found to succeed at describing well the energy dependence of multiparticle observables for RHIC, Tevatron, as well as LHC data [48]. In the HIJING/B$\bar{\mathrm{B}}$ v2.0 model the rapid growth of $dN_{ch}/d\eta$ at mid-rapidity with energy is due to the interplay of copious minijet production with increasing strong color field contributions. However, the large (strange)baryon-to-meson ratios recently measured at LHC energies, especially at $\sqrt{s} = 7$ TeV, are not well described using this set of parameters.

In this work we will address this question and in addition we will discuss a possible dependence of the strength of strong color field on the event multiplicity. We will show that the model predicts a very strong enhancement of (multi)strange baryon-to-meson ratios in HM events. If observed, this could be interpreted as a possible signature for formation of a deconfined but out of local thermal equilibrium mini quark-gluon plasma.

II. THE EFFECTIVE STRING TENSION: AN INFRARED SENSITIVE DYNAMICAL VARIABLE

For a uniform chromo-electric flux tube with field (E), the pair production rate [40, 43] per unit volume for a (light)heavy quark (Q) is given by

$$\Gamma = \frac{\kappa^2}{4\pi^3} \exp\left(-\frac{\pi\, m_Q^2}{\kappa}\right), \tag{1}$$

where $Q = \mathrm{qq}$ (diquark), s (strange), c (charm) or b (bottom). The *current quark masses* are $m_{\mathrm{qq}} = 0.45$ GeV [44], $m_s = 0.12$ GeV, $m_{\mathrm{c}} = 1.27$ GeV, and $m_b = 4.16$ GeV [45]. The *constituent quark masses* of light non-strange quarks are $M_{u,d} = 0.23$ GeV, of the strange quark is M_s=0.35 GeV [46], and of the diquark is $M_{\mathrm{qq}} = 0.55 \pm 0.05$ GeV [44].

An enhanced rate for spontaneous pair production is naturally associated with "*strong chromo-electric fields*", such that $\kappa/m_{\mathrm{Q}}^2 > 1$ *at least some of the time.* In a strong longitudinal color electric field, the heavier flavor suppression factor $\gamma_{Q\bar{Q}}$ varies with string tension via the well known Schwinger formula [47],

$$\gamma_{Q\bar{Q}} = \frac{\Gamma_{Q\bar{Q}}}{\Gamma_{q\bar{q}}} = \exp\left(-\frac{\pi(M_Q^2 - m_q^2)}{\kappa_0}\right) < 1 \tag{2}$$

for $Q = \mathrm{qq}$, s, c or b and $q = u$, d.

In the model calculations, we assume the following effective masses: $M_{qq}^{\mathrm{eff}} = 0.5$ GeV, $M_s^{\mathrm{eff}} = 0.28$ GeV, and $M_c^{\mathrm{eff}} = 1.30$ GeV. Therefore, the above formula implies a suppression of heavier quark production according to $u : d : \mathrm{qq} : s : c \approx 1 : 1 : 0.02 : 0.3 : 10^{-11}$ for the vacuum string tension $\kappa_0 = 1$ GeV/fm. For a color rope (or cluster), on the other hand, if the *average string tension* value κ increases, the suppression factors $\gamma_{Q\bar{Q}}$ increase (i.e., this implies a higher rate of $Q\bar{Q}$ pair production).

Using the HIJING/B$\bar{\mathrm{B}}$ v2.0 model, we have shown that it is important to consider that high energy $p + p$ collisions can have a substantial contribution from SLCF effects [48]. In the model phenomenology, the degree of collectivity is described by the overlap of individual strings (clusters), quantified by the infrared sensitive variable, the string tension (κ). A reduction mechanism of strange quark suppression was introduced by assuming that the effective string tension increased with increasing reaction energy according to a power law:

$$\kappa = \kappa(s) = \kappa_0\ (s/s_0)^{0.06}\ \mathrm{GeV/fm}, \tag{3}$$

where $\kappa_0 = 1$ GeV/fm is the vacuum string tension value and $s_0 = 1$ GeV^2 is a scale factor. In addition to describing well the energy dependence of charged particle density at mid-rapidity from SPS to LHC energies, we have shown that this dynamical mechanism improves the description of the strange meson/hyperon data at Tevatron and LHC energies [48–50]. However, using a set of parameters corresponding to those obtained from Eq. 3, results in an over-prediction of the recently measured yields [29–32] of Ξ particles (by up to a factor of two) and of Ω particles (by up to a factor of four).

A possible reason for this could be a too strong energy dependence used for the mean string tension values (see Eq. 3). Therefore, here we consider a weaker energy dependence of the form,

$$\kappa = \kappa(s) = \kappa_0(s/s_0)^{0.04}\mathrm{GeV/fm}, \tag{4}$$

This leads to a value for the mean string tension of $\kappa = \kappa(s) = 1.7$ GeV/fm at 0.9 TeV and $\kappa = \kappa(s) = 2$ GeV/fm at 7 TeV. The results obtained using this new parametrization will be discussed in Section III.

Because the threshold for strange quark production in a deconfined phase (or in a mQGP) is much smaller than in a hadron gas, a larger enhancement in strange particle production has been suggested as an indication of possible mQGP formation [51–53]. Equation 2, which describes strangeness suppression factors $\gamma_{s\bar{s}}$, shows that an increased value κ up to $\kappa \approx 5$ GeV/fm leads to a saturation of suppression factors, $\gamma_{s\bar{s}}$. For example, in $p + p$ collisions at 7 TeV the suppression factor $\gamma_{s\bar{s}}$ increases from 0.4 (corresponding to $\kappa_0 = 1$ GeV/fm) to approximately 0.85 (corresponding to $\kappa = 5$ GeV/fm), and has only a modest further increase up to 0.89 for $\kappa = 8 - 10$ GeV/fm.

Therefore, if we assume a different energy density in MB and HM $p + p$ collision events (corresponding also to a different type of ropes formation) could lead to different effective κ values. The κ value obtained from Eq. 4 $\kappa = \kappa(s) \approx 2\kappa_0$ can be associated with MB events, since it is deduced from inclusive data. For HM events we will assume an extreme value of $\kappa \approx 5\kappa_0$ GeV/fm, which corresponds to a saturation of strangeness suppression factors. To better characterize the sensitivity to the parameter κ, we also present the result corresponding to an intermediate value $\kappa = \kappa(s) \approx 3\kappa_0$.

Note that a value $\kappa \approx 5\kappa_0$ GeV/fm is also supported by recent calculations at finite temperature (T) of potentials associated with a $q\bar{q}$ pair separated by a distance r [54]. The finite temperature (T) form of the $q\bar{q}$ potential has been calculated by means of lattice QCD [55]. At finite temperature, there are two potentials associated with a $q\bar{q}$ pair separated by a distance r: the free energy $F(T, r)$ and internal energy $V(T, r)$. The free and internal energies actually correspond to slow and fast (relative) motion of the charges, respectively [54]. Infrared sensitive variables such as string tension are very helpful to identify specific degrees of freedom of the plasma. Since the confinement of color in non-Abelian theories is due to the magnetic degree of freedom, the magnetic component is expected to be present in the plasma as well [56]. In the presence of the *chromo-magnetic scenario* it was shown that the effective string tension of the free energy $\kappa = \kappa_F$ decreases with T, to near zero at critical temperature (T_c) [54]. In contrast, the effective string tension of the internal energy (corresponding to a fast relative motion of the charges) $\kappa = \kappa_V$ remains nonzero below about $T = 1.3\,T_c$ with a peak value at T_c about 5 times the vacuum tension κ_0 ($\kappa_V = 5\ \kappa_0 = 5$ GeV/fm) [54].

III. RESULTS AND DISCUSSIONS

A. Charged hadron pseudorapidity and transverse-momentum spectra

All details of the HIJING/B$\bar{\text{B}}$ v2.0 model are extensively discussed in the literature [48–50]. Here we focus our analysis at two energies of interest: $\sqrt{s} = 0.9$ TeV and $\sqrt{s} = 7$ TeV, where data for charged particles [57–64] and identified particles [27–35] have been reported for MB events. Except for the new energy dependence of the string tension (Eq. 4), all the other parameters of the models are as in Ref. [48]. Note that this modification also leads to a relatively small increase (approximately 10-12%) for the predicted density of charged particles at mid-rapidity, in comparison with previous results reported in Ref. [48] in the entire energy region of interest. This increase is now also supported by the new experimental data with LHC energy $\sqrt{s} = 7$ TeV [57–64].

Charged hadron multiplicity measurements are the first results of the LHC physics program. The new data on charged particle pseudorapidity distributions [57, 58], over a limited η range for non single diffractive interactions (NSD), are compared to model calculations in

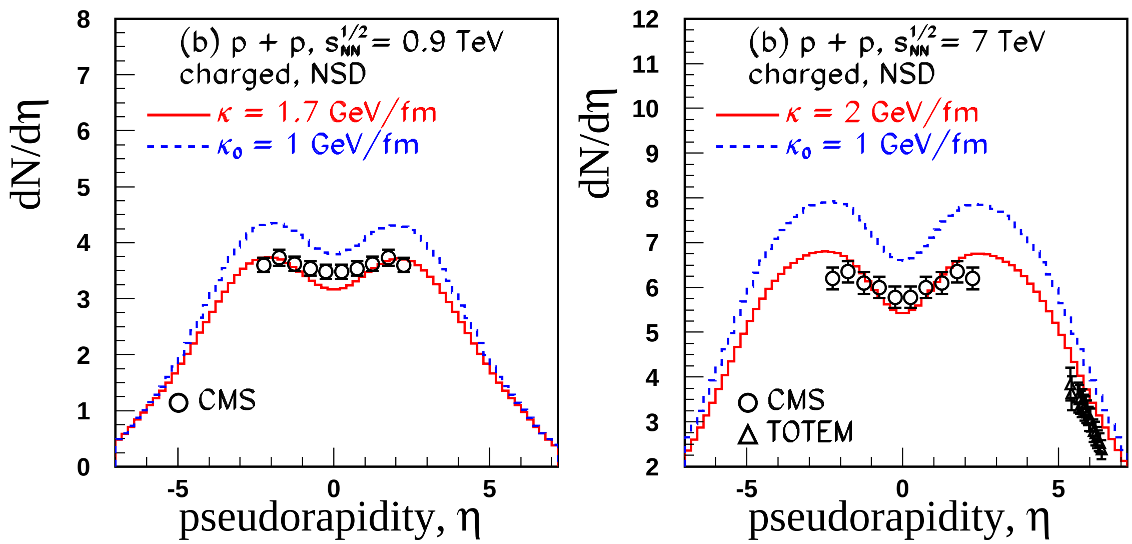

FIG. 1: (Color online) Comparison of HIJING/B$\bar{\text{B}}$ v2.0 predictions for charged particle pseudorapidity distributions at $\sqrt{s} = 0.9$ TeV (left panel) and $\sqrt{s} = 7$ TeV (right panel) for non-single-diffractive (NSD) $p+p$ collisions. The solid and dashed histograms are the results with and without SCF, respectively. The data are from Refs. [57, 58] (CMS) and from Ref. [64] (TOTEM). Only statistical error bars are shown.

Fig. 1. The data show a sizeable increase of the central pseudorapidity density with c.m.s. energy. As the colliding energy increases, the rate of multiple parton interactions (MPI) also increases, producing a rise in the central multiplicity. The increase with energy in our phenomenology is due to the interplay of the increased mini-jet production in high colliding energy with SLCF effects. A scenario with SLCF effects (solid histograms) reproduces well the measured multiplicity distributions. Without SLCF effects (*i.e.*, $\kappa = \kappa_0 = 1$ GeV/fm) the model strongly overestimates the central charged particle density (dashed histograms). Data over a larger rapidity range are needed to determine the shape of the falling density in the fragmentation region. For completeness, the new TOTEM data [64] at forward pseudorapidity are also included.

The measured transverse momentum distributions for NSD events at $\sqrt{s} = 0.9$ TeV and $\sqrt{s} = 7$ TeV are shown in Fig. 2 in the range $0 < p_T < 5$ GeV/c, where both hard and soft processes are expected to contribute. The data of CMS [57, 58] and ATLAS [63] are measured in larger pseudorapidity intervals $|\eta| < 2.5$ and $|\eta| < 1$, respectively. In contrast, ALICE measurements [60] are in a very central region $|\eta| < 0.8$. The calculations were

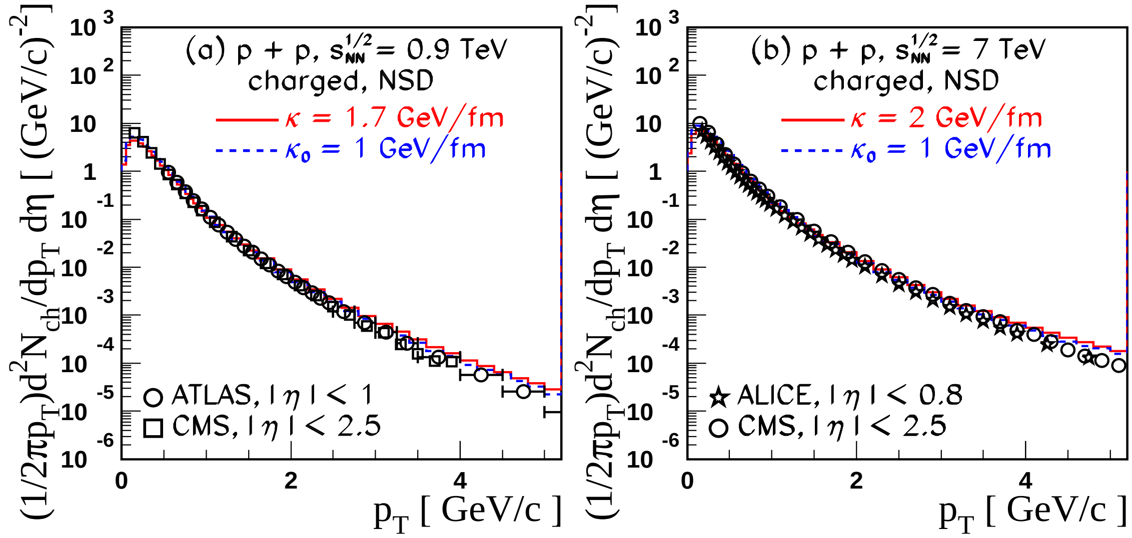

FIG. 2: (Color online) Comparison with data of HIJING/B$\bar{\text{B}}$ v2.0 predictions of charged-hadron transverse momentum distributions ($|\eta| < 0.8$) at LHC energies. The calculated spectra include the combined effects of SLCF and J$\bar{\text{J}}$ loops. The solid and dashed histograms have the same meaning as in Fig. 1. The data are from Refs. [57, 58] (CMS), [60] (ALICE preliminary), [63] (ATLAS). Statistical error bars on the data points are smaller than the markers.

performed using ALICE acceptance but, as can inferred from the data shown in Fig. 1, the difference in pseudorapidity range has a negligible effect on the p_T spectra. The model calculations including SLCF effects give a good description of the spectral shape at low p_T ($p_T < 4$ GeV/c) for both energies. At high p_T ($p_T > 5$ GeV/c) the calculations lead to a somewhat harder spectrum than that observed. In our phenomenology this could indicate that jet quenching, *i.e.*, suppression of high p_T particles like that observed at RHIC energies in nucleus-nucleus collisions, could also appear in $p+p$ collisions, particularly for events with large multiplicity [48].

B. Minimum Bias events. Identified Particle Spectra and Ratios.

The pp single particle inclusive p_T spectra measurements are important for understanding collision dynamics, since the various particles show different systematic behavior, as observed at RHIC energy [65]. Detailed theoretical predictions for single inclusive hadron production (including hyperons) are discussed in this section. Baryon-to-meson ratios are experimental observables that can be used at the LHC to investigate multi-parton interactions and help understanding of the underlying physics [66, 67]. Unexpectedly high ratios observed in $A+A$ collisions at RHIC energies have been discussed in terms of recombination and coalescence mechanisms [68–70]. In $p+p$ collisions, however, a coalescence/hadronization scenario is not favored due to low phase space density in the final state. The HIJING/B$\bar{\text{B}}$ model [48, 50], with SLCF effects and junction-anti-junction ($J\bar{J}$) loops included, provides an alternative dynamical explanation of the heavy-ion data at RHIC energies. We have shown that the model also predicts an increasing yield of (multi)strange particles, thereby better describing the experimental data in $A+A$ and $p+p$ collisions.

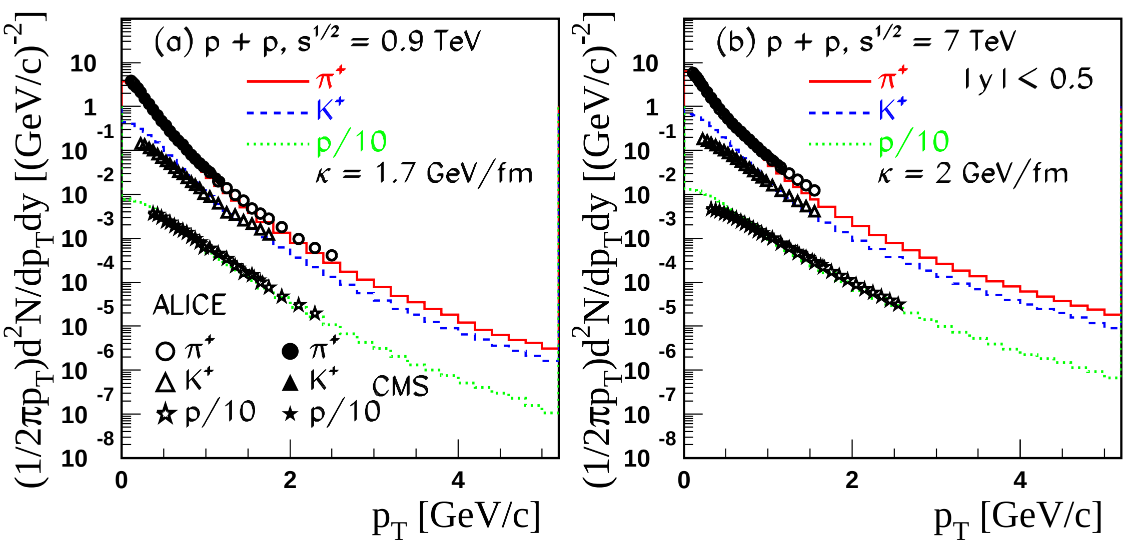

FIG. 3: (Color online) HIJING/B$\bar{\text{B}}$ v2.0 predictions of transverse momentum spectra at mid-rapidity ($|y| < 0.5$) for mesons (π, K) and baryons (p) at $\sqrt{s} = 0.9$ TeV (left panel) and at $\sqrt{s} =$ 7 TeV (right panel) are compared to data. The data (open symbols, left panel) are from Ref. [28] (ALICE). The preliminary data (open symbols, right panel) are from Ref. [29] (ALICE). Preliminary data (closed symbols) are from CMS collaboration and are plotted using a normalization factor 0.78 discussed in Ref. [35]. Statistical error bars on the data points are smaller than the markers. For clarity the data and theoretical calculations for the proton results are divided by a factor of ten.

Figure 3 compares the ALICE results to the predicted mid-rapidity spectra for positive pions (solid histograms), kaons (dashed histograms), and protons (dotted histograms) in minimum bias $p+p$ collisions. There is agreement in the p_T region of interest $1 < p_T < 4$

GeV/c at both energies. The over-prediction for proton and kaon production below $p_T = 1$ GeV/c is consistent with possible presence of radial flow, which seems to be larger at 7 TeV than at 0.9 TeV. The radial flow could appear as a consequence of a hydrodynamic type evolution with flux tube initial conditions [6], not embedded in our model.

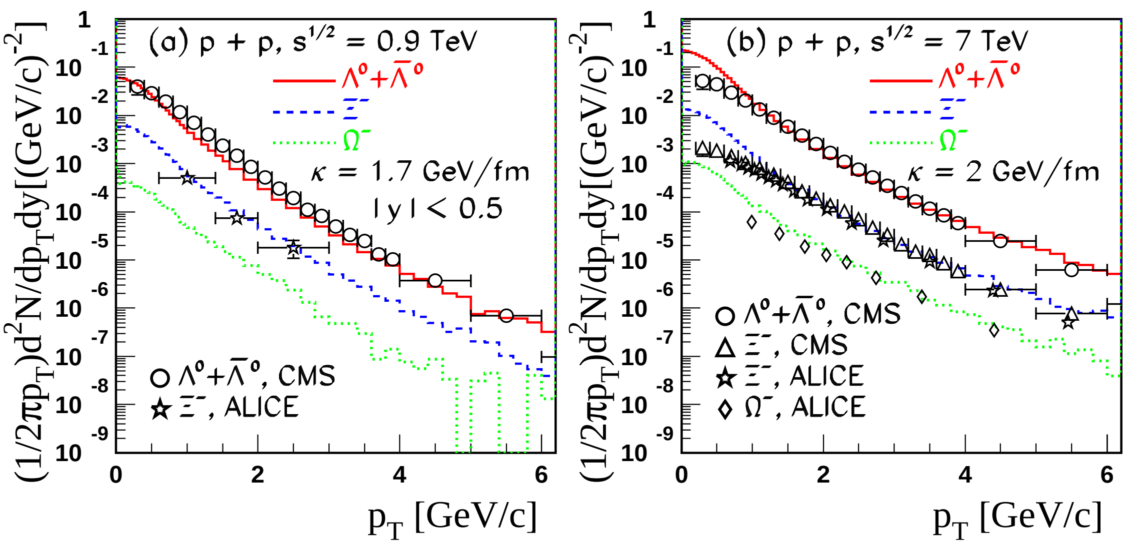

FIG. 4: (Color online) HIJING/B$\bar{\mathrm{B}}$ v2.0 predictions of transverse momentum spectra at mid-rapidity ($|y| < 0.5$) for (multi)strange hyperons (Λ, Ξ, Ω) at $\sqrt{s} = 0.9$ TeV (left panel) and at $\sqrt{s}$ = 7 TeV (right panel) are compared to data. The data are from the ALICE [27, 32] and CMS collaborations [33]. Error bars include only the statistical uncertainties.

We extend our analysis to the production of (multi)strange baryons. In Fig. 4 we show the HIJING/B$\bar{\mathrm{B}}$ v2.0 model predictions of p_T spectra at mid-rapidity ($|y| < 0.5$) for Λ (solid histograms), Ξ^- (dashed histograms) and Ω^- (dotted histograms) baryons at 0.9 TeV and 7 TeV. For (multi)strange particles, the data indicate a stronger radial flow at 7 TeV than at 0.9 TeV. For the p_T region of interest, $1 < p_T < 4$ GeV/c, the model results are in agreement with data at both energies.

Figure 5 shows a comparison of model predictions with ALICE data [28, 29] of non-strange baryon over meson ratios ($\bar{p}/\pi^-$) at 0.9 TeV and 7 TeV. The ratios have been calculated by dividing the spectra reported in Refs. [28, 29]. Within our phenomenology the measured ratios are reasonably described in a scenario with SCLF effects (solid histograms). The larger string tension parameterization results in a predicted increase of the ratio $\bar{p}/\pi^-$ by a factor of ≈ 5 at 7 TeV. Note that the models PYTHIA [36, 37] and EPOS [71, 72] cannot reproduce the observed high baryon-to-meson ratios (see Fig. 6 and Fig. 7 in Ref. [66]).

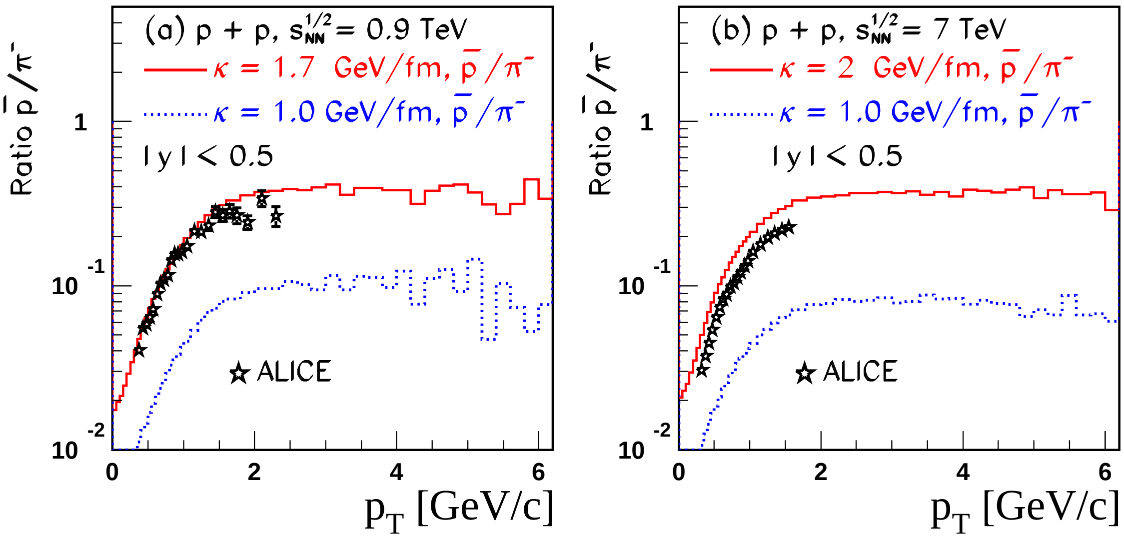

FIG. 5: (Color online) Comparison of HIJING/B$\bar{\text{B}}$ v2.0 predictions with data on the non-strange baryon over meson ratios from minimum bias events in the rapidity range $|y| < 0.5$ at $\sqrt{s} = 0.9$ TeV (left panel) and at $\sqrt{s} = 7$ TeV (right panel). The solid and dashed lines have the same meaning as in Fig. 1. Experimental results at 0.9 TeV are from Ref. [28] (ALICE) and at 7 TeV from Ref. [29](ALICE preliminary). The ratios have been calculated by us, dividing the spectra from Fig. 3. Error bars include only the statistical uncertainties.

The strange-particle ratios could also reveal manifestations of new collective phenomena. In the EPOS model such an increase is obtained if the production of a *mini-plasma* is assumed in $p+p$ collisions [5], [72]. If confirmed by future measurements, these observables could open a perspective on new physics in pp interactions.

To investigate possible differences in the production mechanisms of multi-strange baryons that do or do not contain a non-strange quark we study the ratio of $\Omega^-(sss)$-to-$\Xi^-(dss)$ as a function of transverse momentum, p_T. Due to low statistics we will consider the combined ratio $(\Omega^- + \overline{\Omega}^+)$-to-$(\Xi^- + \overline{\Xi}^+)$ at 7 TeV: the predictions are shown in Fig. 6a. The model results without SLCF effects (dashed histogram) underestimate the data by a factor of approximately 3. Note that recent calculations with the PYTHIA event generator [37–39] strongly underestimate the production rates [33] and fail to describe the above ratio [31]. In contrast, the HIJING/B$\bar{\text{B}}$ v2.0 model in a scenario with SLCF effects (solid histograms) does describes the data. This ratio could also help to study the possible saturation of the

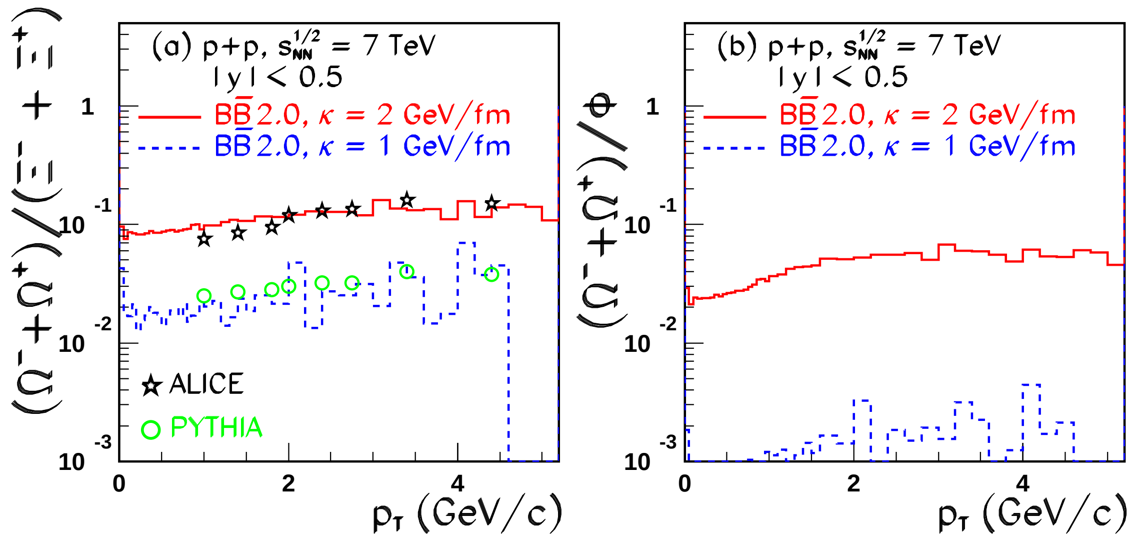

FIG. 6: (Color online) HIJING/B$\bar{\rm B}$ v2.0 predictions of multi-strange hyperon ratios in $p+p$ collisions at $\sqrt{s} = 7$ TeV for ratio Ω/Ξ (left panel) are compared to data. The calculated ratios (solid histogram) include the combined effects of SCF and J$\bar{\rm J}$ loops. The dashed histogram are the results without SCF effects. PYTHIA simulation results from Ref. [31] are also included (left panel). The data are from Ref. [32] (ALICE). Statistical error bars on the data points are smaller than the markers. The model predictions for the ratio of multi-strange hyperons to mesons Ω/ϕ (right panel).

s-quarks, which would be indicated by a flattening at high p_T. However, the currently available data do not allow for firm conclusions.

It has been argued that strangeness production could be suppressed in $p+p$ collisions by the limited volume of the colliding system, which requires localized strangeness conservations [74]. Such a canonical suppression does not, however, explain the suppression of the ϕ meson production in $p+p$ collisions because ϕ has a net strangeness of zero [75, 76]. The study of the Ω/ϕ ratio is therefore also of great interest to distinguish between possible dynamical production mechanisms. The HIJING/B$\bar{\rm B}$ v2.0 model predictions are presented in Fig. 6b. The results predict a strong increase (up to an order of magnitude) for the scenario that includes SLCF effects (solid histogram).

In our approach, the dynamical mechanism that leads to such high values of baryon-to-meson ratios is SLCF appearing at the initial stage of the interaction. The SLCF mechanism strongly modifies the fragmentation processes (strangeness suppression factors) and thus results in a large increase of (strange)baryons. This interpretation is also supported by more sophisticated theoretical calculations, in a scenario in which a time-dependent pulse for the initial strength of the color field is considered [73]. An observed large enhancement of the baryon-to-meson ratios would be consistent with SLCF playing an important role in multiparticle production in $p+p$ collisions at LHC energies and suggesting that high energy density fluctuations can reach very high densities, potentially comparable to those reached in central Au + Au collisions at RHIC energies [1].

C. Baryon-to-meson ratio in HM pp collision events

To test the above assumptions, and in order to study possible new phenomena in $p+p$ collisions, we examine in this paper the dependence of particle production as a function of the total charged particle multiplicity (N_{ch}) and compare the results with those from minimum bias event selection. The MB event selection is defined here as the existence of one charged particle in the rapidity interval $|y| < 1$. Since (multi)strange particle production in heavy-ion reactions is enhanced relative to that in MB $p+p$ collisions [50], one might ask whether the production rates in HM $p+p$ collisions may already exhibit any feature like an enhancement due to SLCF effects. The increase is quantified by calculating the p_T dependence at mid-rapidity ($|y| < 0.8$) of the baryon/meson yield ratios, *e.g.*, (multi)strange baryon (Λ, Ξ, and Ω) over mesons (pions).

Figure 7 shows the model predictions for various baryon-to-meson ratios as a function of transverse momentum. Shown are the results for non-strange baryon over non-strange meson production [$(p+\bar{p})/(\pi^+ + \pi^-)$, part (a)], strange baryon over non-strange meson production [$(\Lambda + \bar{\Lambda})/(\pi^+ + \pi^-)$, part (b)] multi-strange baryon over non-strange meson production [$(\Omega^- + \Omega^+)/(\pi^+ + \pi^-)$, part (c)], and multi-strange baryon over ϕ mesons [$(\Omega^- + \Omega^+)/2\phi$, part (d)] for MB and HM ($N_{\mathrm{ch}} > 120$) events. The results are presented for two scenarios: MB and HM ($N_{\mathrm{ch}} > 120$) events assuming κ= 2 GeV/fm, and for HM events assuming $\kappa = 5$ GeV/fm.

One first notes that, for a constant value of κ, there are negligible differences between the predicted ratios for MB and HM events. On the contrary, assuming a larger value of κ leads to large increases that depend on particle species. The ratio of non-strange baryon over non-strange mesons $(p+\bar{p})/(\pi^+ + \pi^-))$ shows a multiplicative enhancement of approximately 3

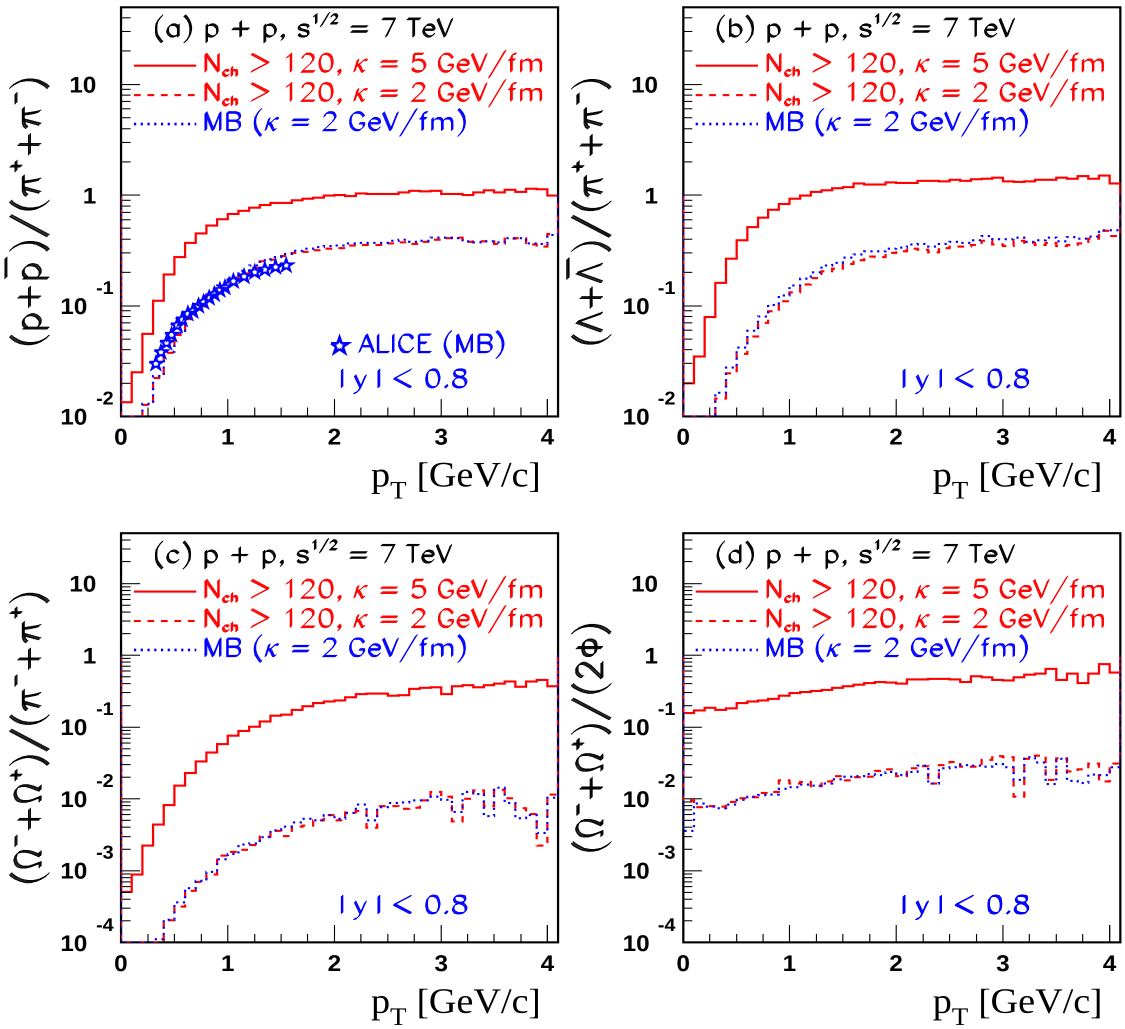

FIG. 7: (Color online) The HIJING/B$\bar{\text{B}}$ v2.0 model predictions for production ratios $[(p+\bar{p})/(\pi^+ + \pi^-)$, (a)], $[(\Lambda + \bar{\Lambda})/(\pi^+ + \pi^-)$, (b)] $[(\Omega^- + \Omega^+)/(\pi^+ + \pi^-)$, (c)] $[(\Omega^- + \Omega^+)/2\phi$, (d)]. The results are plotted at mid-rapidity ($|y| < 0.8$) taking $\kappa = 2$ GeV/fm in the MB event selection (dotted histograms) and HM events with $N_{\rm ch} > 120$ (dashed histograms). For the HM events selection the predictions are also shown considering $\kappa = 5$ GeV/fm (solid histograms). The experimental ratios in (a) have been calculated by dividing the spectra from Ref. [29].

relative to MB and HM results with κ= 2 GeV/fm (Fig 7 a). However, the enhancement for (multi)strange baryon over meson ratio increases with increasing mass of hyperons: up to a factor of four for $(\Lambda + \bar{\Lambda})/(\pi^+ + \pi^-)$ (Fig. 7 b), up to a factor of ten for $(\Xi^- + \Xi^+)/(\pi^+ + \pi^-)$ (not shown here), and up to a factor of twenty for $(\Omega^- + \Omega^+)/(\pi^+ + \pi^-)$ (Fig. 7 c) and $(\Omega^- + \Omega^+)/2\phi$ (Fig. 7 d).

Recently, new (preliminary) data for the ratio of non-strange baryons over mesons, $(p+\bar{p})/(\pi^+ + \pi^-)$ as function of charged particle multiplicity have been reported by the CMS collaboration[35]. These data do not show a dependence of the measured ratio on the multiplicity of the event, consistent with a scenario assuming a constant value for κ. However, the measurements are performed within a very limited p_T range ($p_T < 1.2$ GeV/c) and the selection of events is neither NSD nor INEL and make comparison with theory difficult. Data on (multi)strange particle production extending over a larger p_T range are more sensitive to SCF and would allow drawing a more definitive conclusion.

With high statistics measurements of identified particles, the LHC collaborations could test the model predictions and lend credence to the idea that new phenomena or possible out of equilibrium mQGP has been formed in HM $p+p$ collisions. Note that the ALICE collaboration recently reported measurements of the inclusive J/ψ yield as a function of charged particle density at mid-rapidity ($|\eta| < 1$) in MB and HM events at 7 TeV. HM events were selected with different bins, up to four times MB multiplicity density. In these HM events an enhancement by a factor of about eight for J/ψ yields at mid-rapidity ($|y| < 0.9$) was found relative to those in MB events [77].

Preliminary ALICE data [78] on Λ and K_S^0 nuclear modification factors in central 0-5% Pb+Pb collisions at 2.76A TeV appear also to agree qualitatively with our predictions of enhanced hyperon/meson yield ratios and their nuclear quenching pattern at transverse momentum $p_T > 2$ GeV/c (see Fig. 8 from Ref. [50]). In this paper we propose that a similar enhancement of the baryon-to-meson ratios may be observed in rare HM $p+p$ collisions. Just as in the Pb+Pb collisions, the hyperon/meson enhancement and the quenching pattern of Λ, K_S^0 and $\pi^{\pm}$ in HM $p+p$ collision events relative to those in MB, corroborated with other bulk flow correlations, could provide further evidence of out of equilibrium mQGP production in rare HM $p+p$ reactions.

A mini quark-gluon plasma differs from the strong coupling plasma (sQGP) produced in central nucleus-nucleus ($A+A$) collisions, mostly by its small initial transverse size $R_p \sim 1$ fm compared to the significantly larger nuclear transverse size $R_A \sim 5$ fm. Extensive hydrodynamic [79] and transport calculations [80] have shown that collective flow signatures, such as perfect fluid elliptic flow, require several fm/c to develop. Similarly, jet quenching observables depend strongly on the jet path length and thus, in $p+p$ collisions quenching will be much weaker than in Pb+Pb central collisions. In contrast, signatures associated with strangeness equilibration [50],[52] are generated on much faster time scales. Therefore, hyperon-to-meson ratios and their p_T dependence may serve as the best probe of possible out of equilibrium mQGP formation.

In order to explore better the enhancement of the baryon/meson production ratio as a possible signature of mQGP in p+p collisions, and especially its possible dependence on event multiplicity, the particle yields at mid-rapidity ($|y| < 0.8$) are studied in six bins of charged particle multiplicity: $10 \leq N_{\rm ch} < 30$; $30 \leq N_{\rm ch} < 60$; $60 \leq N_{\rm ch} < 80$; $80 \leq N_{\rm ch} < 100$; $100 \leq N_{\rm ch} < 120$; $N_{\rm ch} \geq 120$.

We select an experimental observable that would be sensitive to possible new phenomena and is well adapted to the low statistics expected from low yield particle production. We consider the integrated values Y_κ of the baryon-to-meson yield ratios shown in Fig. 7. The domain of the integration is taken over the range $1 < p_T < 4$ GeV/c, where the increase appears to be strongest. The calculations of Y_κ are performed for the above six bins of multiplicity. We also define $Y_{\rm MB}$ for MB events, *i.e.*, the integrated ratio without selection on multiplicity. For $Y_{\rm MB}$ the mean value of the string tension is taken as $\kappa = \kappa(s) \approx 2$ GeV/fm. For the multiplicity bins, the calculations are performed for both $\kappa = \kappa(s) \approx 2$ GeV/fm (Y_2) and $\kappa = 5$ GeV/fm (Y_5). Since we expect a gradual transition as function of multiplicity an intermediate value $\kappa = 3$ GeV/fm (Y_3) is also considered.

In Figure 8, the theoretical predictions for the relative increase in the integrated values Y_κ to the integrated values $Y_{\rm MB}$, *i.e.*, the ratio $R_\kappa = Y_\kappa/Y_{\rm MB}$, are shown. Note that the statistical fluctuations are too large in the first bin ($10 \leq N_{\rm ch} < 30$) so it is not included in the plot. The calculations are presented for the ratios $R_2 = Y_2/Y_{\rm MB}$, $R_3 = Y_3/Y_{\rm MB}$, and $R_5 = Y_5/Y_{\rm MB}$.

As examples, the predictions for (multi)strange-baryon-to-meson ratios are given, *i.e.*, $(\Lambda + \bar{\Lambda})/(\pi^+ + \pi^-)$ and $(\Omega^- + \Omega^+)/(\pi^+ + \pi^-)$. For the $(\Lambda + \bar{\Lambda})/(\pi^+ + \pi^-)$ ratio, the model predicts an almost constant value of R_κ with no multiplicity dependence, while a slight dependence is predicted for the ratio R_5 of $(\Omega^- + \Omega^+)/(\pi^+ + \pi^-)$. For the ratio $(\Lambda + \bar{\Lambda})/(\pi^+ + \pi^-)$ an enhancement of a factor of 4 of R_5 over R_2 is predicted (Fig. 8a). In contrast, for $(\Omega^- + \Omega^+)/(\pi^+ + \pi^-)$ (Fig. 8b) higher values (up to a factor of approximately 40) are predicted in the scenario with a possible transition to an out of equilibrium mQGP state, R_5 (solid line), than in a scenario without, R_2 (dotted line).

If the assumption of the dependence of κ on the total charged particle multiplicity ($N_{\rm ch}$) is

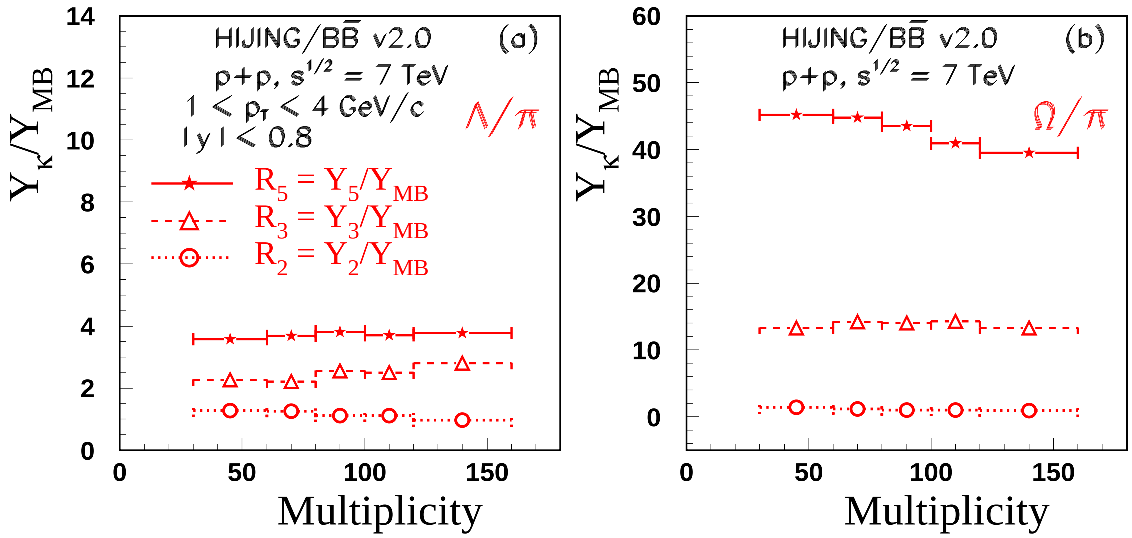

FIG. 8: (Color online) HIJING/B$\bar{\text{B}}$ v2.0 predictions for the relative increase $R_\kappa = Y_\kappa/Y_{\text{MB}}$ (see text for explanation). The results are plotted as a function of multiplicity in five bins: $30 \leq N_{\text{ch}} < 60$; $60 \leq N_{\text{ch}} < 80$; $80 \leq N_{\text{ch}} < 100$; $100 \leq N_{\text{ch}} < 120$; $N_{\text{ch}} > 120$. The values R_κ are given for $(\Lambda + \bar{\Lambda})/(\pi^+ + \pi^-)$ (left panel) and for $(\Omega^- + \Omega^+)/(\pi^+ + \pi^-)$ (right panel). The results for the relative increase $R_3 = Y_3/Y_{\text{MB}}$ (triangles) and $R_5 = Y_5/Y_{\text{MB}}$ (stars) are obtained using $\kappa = 3$ GeV/fm and $\kappa = 5$ GeV/fm, respectively. The integrated values Y_{MB} are obtained using $\kappa = \kappa(s) \approx 3$ GeV/fm [48].

valid, we expect to see in the data a transition from R_2 (dotted line) at low multiplicity to R_3 (dashed line), to R_5 values (solid line) for higher multiplicity events. These results strongly suggest that the experimental data could contain a signature for a possible transition to a mQGP phase in hadronic collisions. The shape of an observed transition as a function of multiplicity could contain information on the nature of the underlying physics, *e.g.*, if the transition is smooth or has a net threshold.

We showed that the baryon-to-meson ratios have an enhancement up to the highest LHC energy (14 TeV) [48]. Based on Eq. 4 the string tension value has a predicted modest increase from ≈ 2 GeV/fm to ≈ 2.15 GeV/fm, when going from $\sqrt{s} = 7$ TeV to $\sqrt{s} = 14$ TeV. In addition, as shown in Ref. [48], a saturation sets in near $\sqrt{s} \approx 3$ TeV. Therefore, we expect relatively small further increases in the strange particle ratios and in the predicted values for R_κ in HM $p + p$ collisions at higher LHC energy.

IV. CONCLUSIONS

In this work within the phenomenology of the HIJING/B$\bar{\text{B}}$ v2.0 model we discussed observables sensitive to possible new phenomena, such as strong longitudinal color fields in HM $p + p$ collision events. For MB bias events we show that a good description is obtained for charged and identified particle production, taking an energy dependence of mean string tension values $\kappa = \kappa(s) = \kappa_0(s/s_0)^{0.04}$ GeV/fm.

The predictions for baryon/meson production ratios in $p + p$ collisions at $\sqrt{s} = 7$ TeV are discussed. We analyze the dependence of these ratios on the degree of collectivity in the reaction dynamics, characterized by an infrared sensitive variable, the string tension κ. The formation of a collective phase in high multiplicity $p + p$ collisions would be made evident within our phenomenology by a relative increase in the baryon/meson ratios with increasing multiplicity, particularly those ratios involving strange and multi-strange particles.

The experimental data could show a multiplicity dependent transition as indicated by comparing results obtained with a lower value of $\kappa = 2$ GeV/fm to those corresponding to a higher value of $\kappa = 5$ GeV/fm originating from possible production of a transitory out of equilibrium mQGP phase. This transition is most likely gradual as a function of multiplicity and center-of-mass energy $\sqrt{s}$. Corroborated with other observables sensitive to collective behavior, such as *ridge structure*, enhanced radial flow, high p_T particle suppression (*jet quenching*) in $p + p$ collisions, observation of saturation of hyperon/meson ratios could provide possible signatures of out of equilibrium mQGP phase formed in high multiplicity $p + p$ collision events at ultra-high energies.

V. ACKNOWLEDGMENTS

Acknowledgments: We thank S. Das Gupta for useful discussions and continue support. VTP acknowledges discussion with M. Petrovici and access to computer facilities IFIN-HH, Bucharest, Romania and at Columbia University, New York, where parts of these calculations were performed. This work was supported by the Natural Sciences and Engineering Research Council of Canada. This work was also supported by the Division of Nuclear Science, of the U. S. Department of Energy under Contract No. DE-AC03-76SF00098 and

DE-FG02-93ER-40764.

---

[1] B. Alver *et al.* (PHOBOS Collaboration), Phys. Rev. C **83**, 024913 (2011).

[2] J. D. Bjorken, Phys. Rev. D **27**, 140 (1983).

[3] S. S. Adler *et al.* (PHENIX Collaboration), Phys. Rev. C **71**, 034908 (2005), [Erratum-ibid. C **71**, 049901 (2005).]

[4] J. D. Bjorken, Preprint FERMILAB-PUB-82-059-THY (1982).

[5] N. Armesto, N. Borghini, S. Jeon, U. A. Wiedemann (eds.), S. Abreu, V. Akkelin, J. Alam and J. L. Albacete *et al.*, J. Phys. G **35**, 054001 (2008).

[6] K. Werner, I. Karpenko, T. Pierog, M. Bleicher and K. Mikhailov, Phys. Rev. C **83**, 044915 (2011).

[7] L. Cunqueiro, J. Dias de Deus and C. Pajares, Eur. Phys. J. C **65**, 423 (2010).

[8] A. Kisiel, Phys. Rev. C **84**, 044913 (2011).

[9] P. Bozek, Eur. Phys. J. C **71**, 1530 (2011).

[10] H. J. Pirner and K. Reygers, Phys. Rev. D **86**, 034005 (2012).

[11] M. A. Braun, C. Pajares and V. V. Vechernin, arXiv:1204.5829 [hep-ph].

[12] L. Van Hove, Phys. Lett. B **118**, 138 (1982).

[13] Renato Campanini, Gianluca Ferri, Phys. Lett. B **703**, 237 (2011).

[14] F. -M. Liu and K. Werner, J. Phys. G **38**, 124183 (2011).

[15] F. -M. Liu and K. Werner, Phys. Rev. Lett. **106**, 242301 (2011).

[16] V. Khachatryan *et al.* (CMS Collaboration), JHEP **1009**, 091 (2010).

[17] W. Li (CMS Collaboration), J. Phys. G **38**, 124027 (2011).

[18] D. Velicanu (CMS Collaboration), J. Phys. G **38**, 124051 (2011).

[19] G. Aad *et al.* (ATLAS Collaboration), ATLAS-CONF-2011-055, 19^{th} International Workshop on Deep Inelastic Scattering and Related Subjects, 11-15 April, 2011, Newport News, VA, USA

[20] K. Werner, I. Karpenko and T. Pierog, Phys. Rev. Lett. **106**, 122004 (2011).

[21] M. Y. Azarkin, I. M. Dremin and A. V. Leonidov, Mod. Phys. Lett. A **26**, 963 (2011), [Erratum-ibid. A **26**, 1309 (2011).]

[22] R. C. Hwa and C. B. Yang, Phys. Rev. C **83**, 024911 (2011).

[23] A. Dumitru, K. Dusling, F. Gelis, J. Jalilian-Marian, T. Lappi and R. Venugopalan, Phys. Lett. B **697**, 21 (2011).

[24] T. A. Trainor and D. T. Kettler, Phys. Rev. C **84**, 024910 (2011).

[25] E. Shuryak, arXiv:1009.4635 [hep-ph].

[26] G. Aad *et al.* (ATLAS Collaboration), Phys. Rev. D **85**, 012001 (2012).

[27] K. Aamodt *et al.* (ALICE Collaboration), Eur. Phys. J. C **71**, 1594 (2011).

[28] K. Aamodt *et al.* (ALICE Collaboration), Eur. Phys. J. C **71**, 1655 (2011).

[29] M. Chojnacki (ALICE Collaboration), J. Phys. G **38**, 124074 (2011).

[30] M. Floris (ALICE Collaboration), J. Phys. G **38**, 124025 (2011).

[31] D. D. Chinellato (ALICE Collaboration), J. Phys. G **38**, 124079 (2011).

[32] B. Abelev *et al.* (ALICE Collaboration), Phys. Lett. B **712**, 309 (2012).

[33] V. Khachatryan *et al.* (CMS Collaboration), JHEP **1105**, 064 (2011).

[34] R. Rougny, to be published in Proceedings of Hadron Collider Physics Symposium 2011 (HCP 2011),14-18 Nov 2011: Paris, France , arXiv:1201.5563v2 [hep-ex].

[35] V. Khachatryan *et al.* (CMS Collaboration), CMS PAS FSQ-12-014 (2012).

[36] T. Sjostrand, S. Mrenna and P. Z. Skands, Comput. Phys. Commun. **178**, 852 (2008).

[37] T. Sjostrand, S. Mrenna and P. Z. Skands, JHEP **0605**, 026 (2006).

[38] P. Z. Skands, Phys. Rev. D **82**, 074018 (2010).

[39] R. Field, To be published in Proceedings of Hadron Collider Physics Symposium 2010: HCP 2010, 23-27 Aug 2010: Toronto, Ontario, Canada,arXiv:1010.3558[hep-ph].

[40] M. Gyulassy and A. Iwazaki, Phys. Lett. B. **165**, 157 (1985).

[41] F. Gelis, T. Lappi and L. McLerran, Nucl. Phys. **A828**, 149 (2009); T. Lappi and L. McLerran, Nucl. Phys. **A772**, 200 (2006).

[42] L. McLerran, J. Phys. G **35**, 104001 (2008).

[43] T. D. Cohen and D. A. McGady, Phys. Rev. D **78**, 036008 (2008).

[44] M. Cristoforetti, P. Faccioli, G. Ripka, and M. Traini, Phys. Rev. D **71**, 114010 (2005).

[45] K. Nakamura *et al.* [Particle Data Group], J. Phys. G **37**, 075021 (2010).

[46] N. S. Amelin, N. Armesto, C. Pajares, and D. Sousa, Eur. Phys. J. C **22**, 149 (2001).

[47] J. S. Schwinger, Phys. Rev. **82**, 664 (1951).

[48] V. Topor Pop, M. Gyulassy, J. Barrette, C. Gale and A. Warburton, Phys. Rev. C **83**, 024902 (2011).

[49] V. Topor Pop, J. Barrette and M. Gyulassy, Phys. Rev. Lett. **102**, 232302 (2009).

[50] V. Topor Pop, M. Gyulassy, J. Barrette and C. Gale, Phys. Rev. C **84**, 044909 (2011).

[51] P. Koch, B. Muller and J. Rafelski, Phys. Rept. **142**, 167 (1986).

[52] B. Muller, Acta Phys. Polon. B **43**, 761 (2012).

[53] B. Muller, J. Schukraft and B. Wyslouch, arXiv:1202.3233 [hep-ex].

[54] J. Liao and E. Shuryak, Phys. Rev. D **82**, 094007 (2010).

[55] O. Kaczmarek and F. Zantow, Phys. Rev. D **71**, 114510 (2005).

[56] M. N. Chernodub and V. I. Zakharov, Phys. Rev. Lett. **98**, 082002 (2007).

[57] V. Khachatryan *et al.* (CMS Collaboration), JHEP **1002**, 041 (2010).

[58] V. Khachatryan *et al.* (CMS Collaboration), Phys. Rev. Lett. **105**, 022002 (2010).

[59] K. Aamodt *et al.* (ALICE Collaboration), Phys. Lett. B **693**, 53 (2010).

[60] J. Otwinowski (ALICE Collaboration), J. Phys. G **38**, 124112 (2011).

[61] K. Aamodt *et al.* (ALICE Collaboration), Eur. Phys. J. C **68**, 345 (2010).

[62] K. Aamodt *et al.* (ALICE Collaboration), Eur. Phys. J. C **68**, 89 (2010).

[63] G. Aad *et al.* (ATLAS Collaboration), Phys. Lett. B **688**, 21 (2010).

[64] P. Aspell *et al.* (TOTEM Collaboration), Europhys. Lett. **98**, 31002 (2012).

[65] M. J. Tannenbaum, PoS CERP **2010**, 019 (2010).

[66] B. Hippolyte, Eur. Phys. J. C **62**, 237 (2009).

[67] H. Ricaud, A. Kalweit and A. Maire, J. Phys. G **37**, 094049 (2010).

[68] R. J. Fries, B. Muller, C. Nonaka and S. A. Bass, Phys. Rev. C **68**, 044902 (2003).

[69] V. Greco, C. M. Ko and P. Levai, Phys. Rev. C **68**, 034904 (2003).

[70] R. C. Hwa and C. B. Yang, Phys. Rev. C **67**, 034902 (2003).

[71] K. Werner, T. Hirano, I. Karpenko, T. Pierog, S. Porteboeuf, M. Bleicher and S. Haussler, Nucl. Phys. Proc. Suppl. **196**, 36 (2009).

[72] K. Werner, I. Karpenko and T. Pierog, J. Phys. Conf. Ser. **230**, 012026 (2010).

[73] V. Skokov and P. Levai, PoS **EPS-HEP2009**, 456 (2009); P. Levai and V. Skokov, Phys. Rev. D **82**, 074014 (2010);P. Levai, D. Berenyi, A. Pasztor and V. V. Skokov,J. Phys. G **38**, 124155 (2011).

[74] I. Kraus, J. Cleymans, H. Oeschler and K. Redlich, J. Phys. G **37**, 094021 (2010).

[75] F. Becattini, J. Phys. G **36**, 064019 (2009).

[76] N. Xu (STAR Collaboration), J. Phys. G **35**, 044031 (2008).

[77] B. Abelev *et al.* (ALICE Collaboration), Phys. Lett. B **712**, 165 (2012).

[78] S. Schuchman, Work presented at 7^{th} Int. Workshop on High p_T Physics at the LHC, 26-29 March, 2012, Frankfurt, Germany (private communication).

[79] P. F. Kolb and U. W. Heinz, in Quark gluon plasma 3, pp634-714, Rudolph C. Hwa and Xin-Nian Wang (Editors), World Scientific Publishing Co., 2004.

[80] D. Molnar and M. Gyulassy, Nucl. Phys. A **698**, 379 (2002).